Article

Journal of
Nanoscience and Nanotechnology
Vol. 18, 5013–5019, 2018
www.aspbs.com/jnn

Analysis of Laser Injection Condition and Electrical Properties in Local BSF for Laser Fired Contact c-Si Solar Cell Applications

Cheolmin Park[1], Gyuho Choi[2], Nagarajan Balaji[1], Minkyu Ju[2], Youn-Jung Lee[2], Haeseok Lee[3], and Junsin Yi[1, 2, *]

[1] Department of Energy Science, Sungkyunkwan University, Suwon, 440-746, Korea
[2] School of Electronic Electrical Engineering, College of Information and Communication Engineering, Sungkyunkwan University, Suwon, 440-746, Korea
[3] Department of Materials Science and Engineering, Korea University, Anam-Dong 5-1, Seongbuk-gu, Seoul, 136-701, Korea

A crystalline silicon (c-Si) local-back-contact (LBC) solar cell for which a laser-condition-optimized surface-recombination velocity (SRV), a contact resistance (R_c), and local back surface fields (LBSFs) were utilized is reported. The effect of the laser condition on the rear-side electrical properties of the laser-fired LBC solar cell was studied. The Nd:YAG-laser (1064-nm wavelength) power and frequency were varied to obtain LBSF values with a lower contact resistance. A 10-kHz laser power of 44 mW resulted in an R_c of 0.125 ohms with an LBSF thickness of 2.09 μm and a higher open-circuit voltage (V_{OC}) of 642 mV.

Keywords: Crystalline Silicon Solar Cell, Laser Fired Contact, LBSF, SRV.

1. INTRODUCTION

Laser technology is continually improving; systems are steadily becoming faster, more accurate and more reliable. The solar industry can take the advantages of this progress and apply the laser processing to solar cell manufacturing. Laser beam technologies and their application for solar cell processing have a history of at least two decades.[1–9]

An efficient strategy for minimizing the recombination losses of solar cells is to reduce the metal-semiconductor interface area at the contacts and to passivate the remaining surface area by dielectric layers. Point contacts reduce the influence of recombination in the heavily diffused contact regions by limiting their total area. This was traditionally been achieved using expensive photolithographic processing steps. To obtain the low-cost and highly efficient solar cells, it is also crucial to use a reliable technology for realizing openings in passivation layers without damaging the underlying silicon. An example of this strategy is the rear side of PERC (Passivated Emitter Rear Contact) solar cells where a passivation layer at the rear surface was perforated by local contact openings. Sunpower Corporation produces a commercially adapted version of the point contact design without photolithographic processes, achieving efficiencies of over 21%. Another example is the laser fired contact (LFC) technique, developed at the Fraunhofer Institute for Solar Energy Systems. It presents a promising way to reduce the recombination associated with the rear electrode with efficiencies over 20% reported on PERC structures.[3]

Laser-based process to form LFC in solar cell manufacturing has attracted intensive interests. Comparing to conventional technology of screen-printing metallization, LFC not only avoid large mechanical pressure applied on thin wafer, but also reduce the carrier recombination on rear surface. Furthermore, LFC process can be flexibly handled according to users' specific needs. In order to obtain an LFC cell with reasonable performance, laser spot diameter and lasing time needs to be adjust carefully to control lattice temperature of the laser-focused local area. Local profiles of temperature and concentration of the metal atoms generated by laser ablation affect the profile of metal atoms penetrated/diffused into bulk silicon.

Laser condition optimization is the key issue for achieving high efficiency as it could affect the lifetime, surface recombination velocity (SRV), local back surface

*Author to whom correspondence should be addressed.

field (LBSF) concentration, and junction depth due to the laser damage on the rear surface. In this work, *p*-type c-Si solar cells with local back contact (LBC) was fabricated and the relationship between laser condition and contact resistance, junction depth, SRV were studied.

2. EXPERIMENTAL DETAILS

The solar cell was fabricated using *p*-type Cz-Si wafers with thickness of 200 μm and resistivity around 1∼3 Ω-cm with (100) orientation. The rear surface of wafers was protected using texture barrier. The wafers were textured using NaOH etching solution for 25 minutes. All textured *p*-type c-Si wafers were diffused using phosphorus, a pentavalent impurity, by a conventional thermal diffusion process in a furnace using $POCl_3$ as dopant source at 830 °C for 20 minutes. Thin phosphorus-silicate-glass (PSG) coating formed on the surface was removed by dipping the wafer in HF solution. The diffused wafers were annealed at 880 °C for 25 minutes followed by 7 minutes at 830 °C as a drive-in process. Again wafers were doped for 20 minutes at 830 °C.

For front and rear passivation, after RCA clean, the dry oxidation was carried using tube furnace and SiN_x deposition by PECVD. The wafer was loaded into the furnace at 860 °C. The wafer was loaded into the furnace at 860 °C. Waiting time of 10 minutes was taken to stabilize the temperature while the furnace was filled with nitrogen. Once the temperature stabilized at 860 °C, the nitrogen and oxygen were flowed into the furnace with the ratio of 8:2 and the process carried out for 130 minutes resulted in 20∼30 nm thick SiO_2 on both sides of the wafer. When the oxidation process was finished, annealing in the environment of nitrogen to improve the quality of the film. Finally, SiN_x layer was deposited on the front and back-side using PECVD with gas ratio 45:90 of SiH_4 and NH_3.

Front Ag electrodes were formed using screen-printing method. For the back-side electrode, Al was deposited 2 μm by thermal evaporation and then local contacts were formed by laser fired using Nd:YAG laser. The laser power, frequency and contact coverage was varied from 44∼480 mW, 10∼200 kHz and 0.1∼1.5%, respectively. Annealing was carried out to improve the Ohmic contacts. RTP (rapid thermal processing) was done at 400 °C for 15 minutes in the environment of forming gas with 5% hydrogen. After the completion of the solar cell fabrication, the cells were characterized using the Suns-V_{OC} measurement adopting Illuminated Current–Voltage (LIV) characteristics under the global solar spectrum of AM 1.5 at 25 °C. Fabrication sequence of proposed structure is shown in Figure 1.

3. RESULTS AND DISCUSSION

SiO_2 thin film with good passivation effect was grown by high temperature oxidation furnace and then SiN_x is

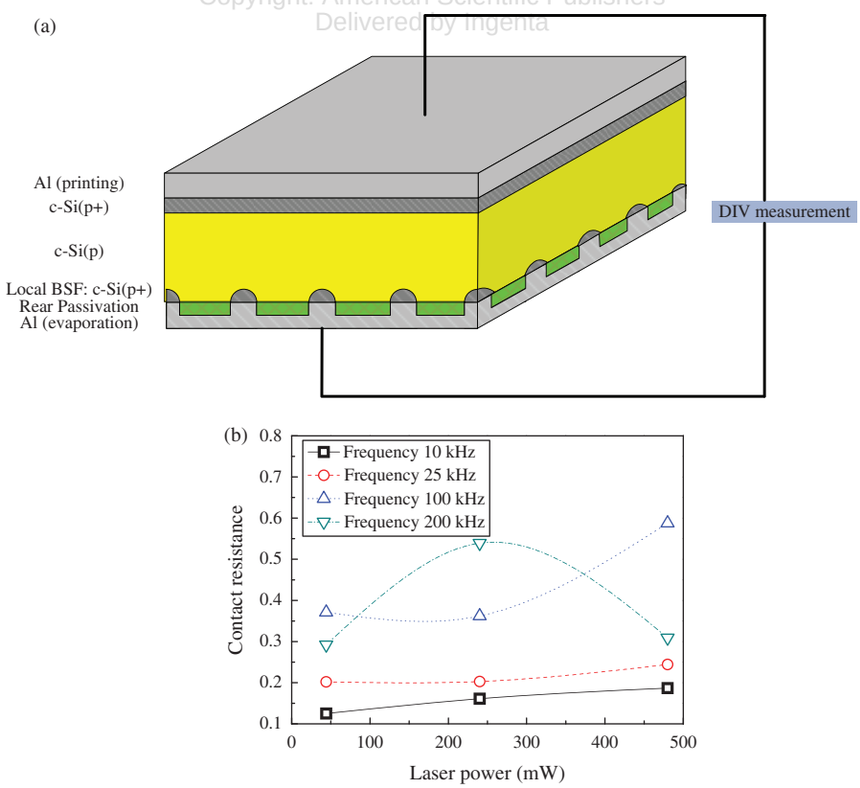

Figure 1. (a) Schematic diagram of contact resistance measurement. (b) Contact resistance under various conditions of laser power and frequency.

deposited on the front side by plasma enhanced chemical vapor deposition (PECVD) while the back side was covered with SiO_2, SiO_2 with FGA or SiO_2/SiN_x. After Forming Gas Annealing (FGA) it decreased to about 30∼50 cm/s and after the deposition of SiN_x, it decreased to about 10∼30 cm/s. For both FGA and SiN_x deposition elevated the passivation quality due to hydrogenation effect.[10] To see the effect of the laser conditions on the actual solar cells, solar cells were fabricated. For back passivation, the thin film of SiO_2/SiN_x which had showed the

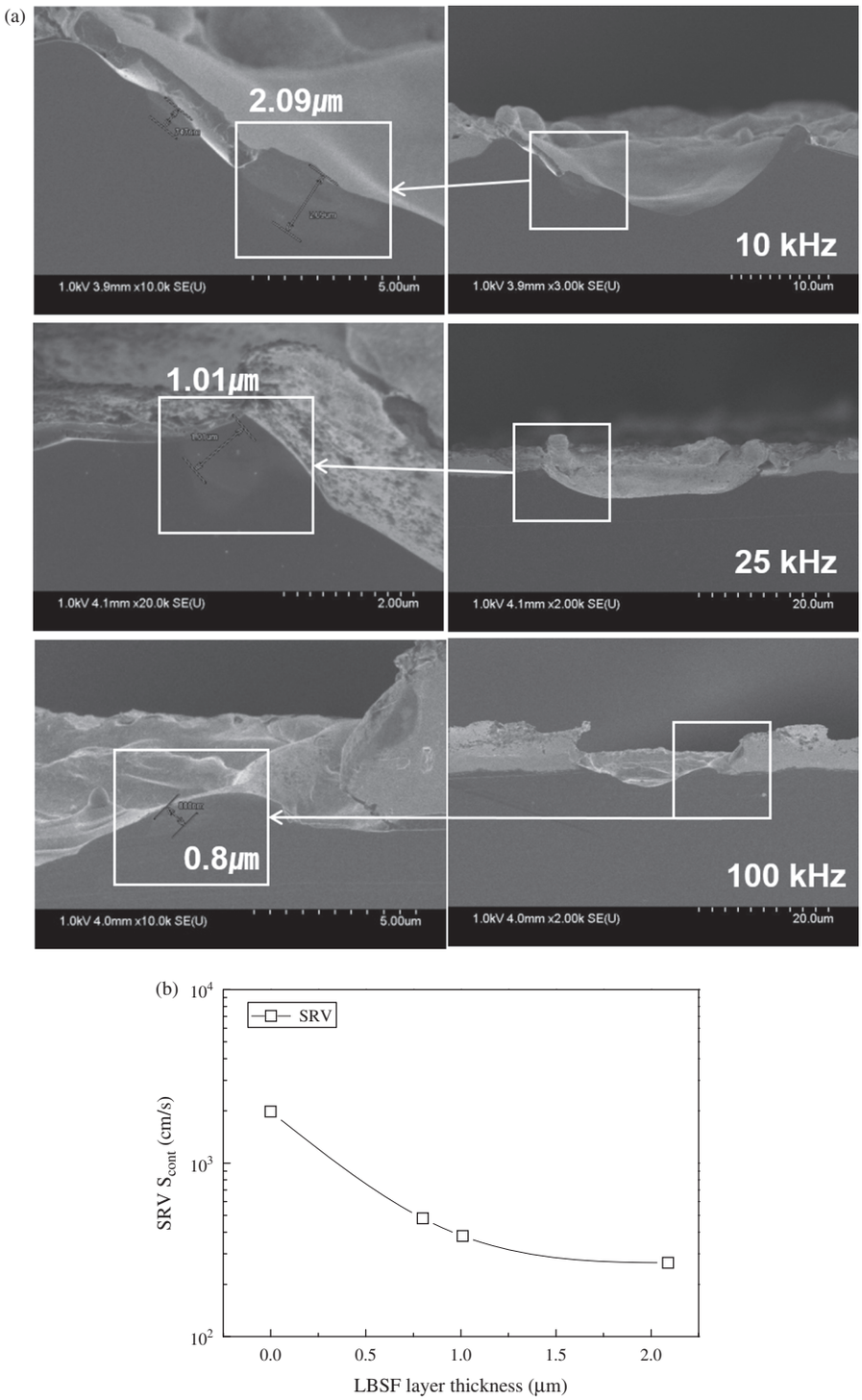

Figure 2. (a) SEM images showing BSF thickness obtained with various laser conditions. (b) SRV dependence on LBSF layer thickness.

best performance was used. For the condition of laser fired contacts, the power was fixed at 1% and the frequency was varied as 10, 25, 100 and 200 kHz.

When the Ohmic contacts are formed, the contact resistance becomes low. Figure 1(a) show the contact resistance of samples with different laser conditions measured through DIV (Dark Current–Voltage) characteristics. For better accuracy, the resistance of probe was measured and subtracted from the results. Figure 1(b) shows the measured contact resistances. As the power and frequency of the laser decreased, the contact resistance also decreased. It can be inferred that the BSF area was larger as the diameter of the dot became larger and that the contact resistance was lower. The low contact resistance means that Ohmic contacts are formed due to the formation of BSF by Si/Al alloy.

To see the depth of BSF formed under different conditions, LV-SEM (Low Vacuum Scanning Electron Microscopy) was taken. The samples used here were the same samples used in the case of O.M. Figure 2(a) shows that the samples with lower resistance had thicker BSF layer.

The effect of local BSF thickness on the solar cells is analyzed more. In *p*-type substrate solar cells, the collection of minority carrier, electrons is very important. The electrons should be collected by the front electrode and the holes should be collected by the back electrode. The p^+ BSF at the back pushes away the electrons to the opposite side by the electric field and makes it easier for the holes to be collected. Thus, the probability of recombination of the electrons and holes becomes less and the current increases. The SRV was obtained through Suns-V_{OC} measurement. Figure 2(b) shows the change in SRV with various LBSF thicknesses. As expected, the values of the SRV beneath the metal contacts (S_{cont}) were low for the samples with formed local BSF. Without local BSF, the value of S_{cont} was 1.98×10^3 cm/s. As the thickness of local BSF

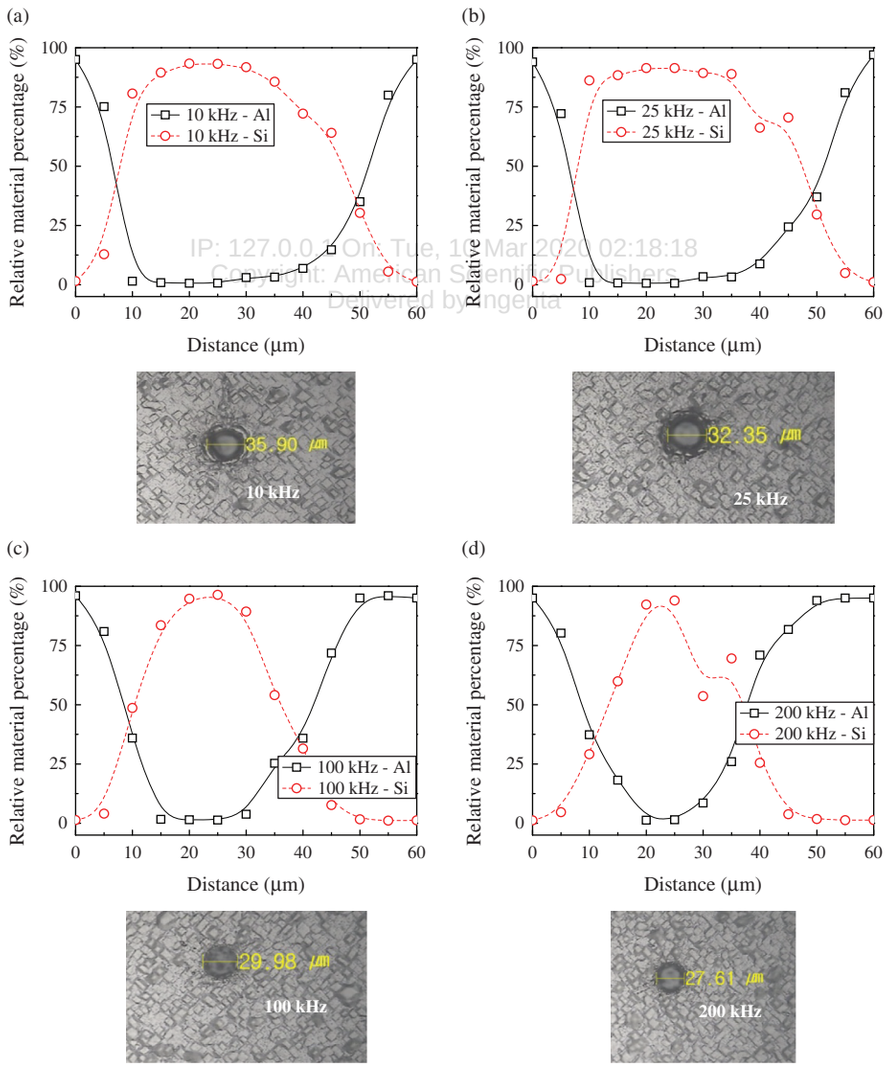

Figure 3. EDS measurements of laser fired contacts with different frequency (a) 10 kHz (b) 25 kHz (c) 100 kHz (d) 200 kHz.

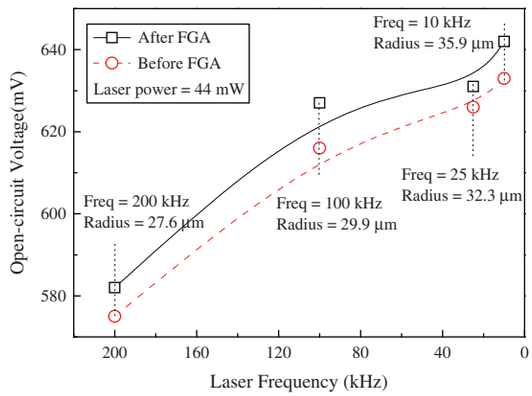

Figure 4. Dependence of open circuit voltage on LBSF layer thickness.

became 2.09 μm, it reduced to 2.65×10^2 cm/s. Assuming ideal diode characteristics the open-circuit voltage of a solar cell can be calculated using the one-diode equation.

$$V_{OC} = \frac{kT}{q} \ln\left(\frac{J_{SC}}{J_{0b} + J_{0e}} + 1\right) \tag{1}$$

where, J_{0b} and J_{0e} is the saturation current density of base and emitter region, respectively. J_{0b} the saturation current density of the base condense all contributions to the saturation current density originating from the rear side as well as from the base material of the solar cell. J_{0b} can be expressed by

$$J_{0b} = \frac{qn_i^2 D_p}{LN_D} \frac{S_{\text{rear, eff}} \cosh(W/L) + (D_p/L)\sinh(W/L)}{(D_p/L)\cosh(W/L) + S_{\text{rear, eff}} \sinh(W/L)} \tag{2}$$

Fischer introduced an analytical model for the calculation of an effective surface recombination velocity of the locally back contacted solar cell on rear side[11]

$$S_{\text{rear, eff}} = \frac{D_p}{W}\left[\frac{p}{2W\sqrt{\pi f}}\arctan\left(\frac{2W}{p}\sqrt{\frac{\pi}{f}}\right) - \exp\left(-\frac{W}{p}\right) + \frac{D_p}{fWS_{\text{cont}}}\right]^{-1} + \frac{S_{\text{pass}}}{1-f} \tag{3}$$

$S_{\text{rear, eff}}$ was shown the effective surface recombination velocity of the rear side, S_{pass} the SRV beneath the passivated area, f the contact coverage (or fraction), p the

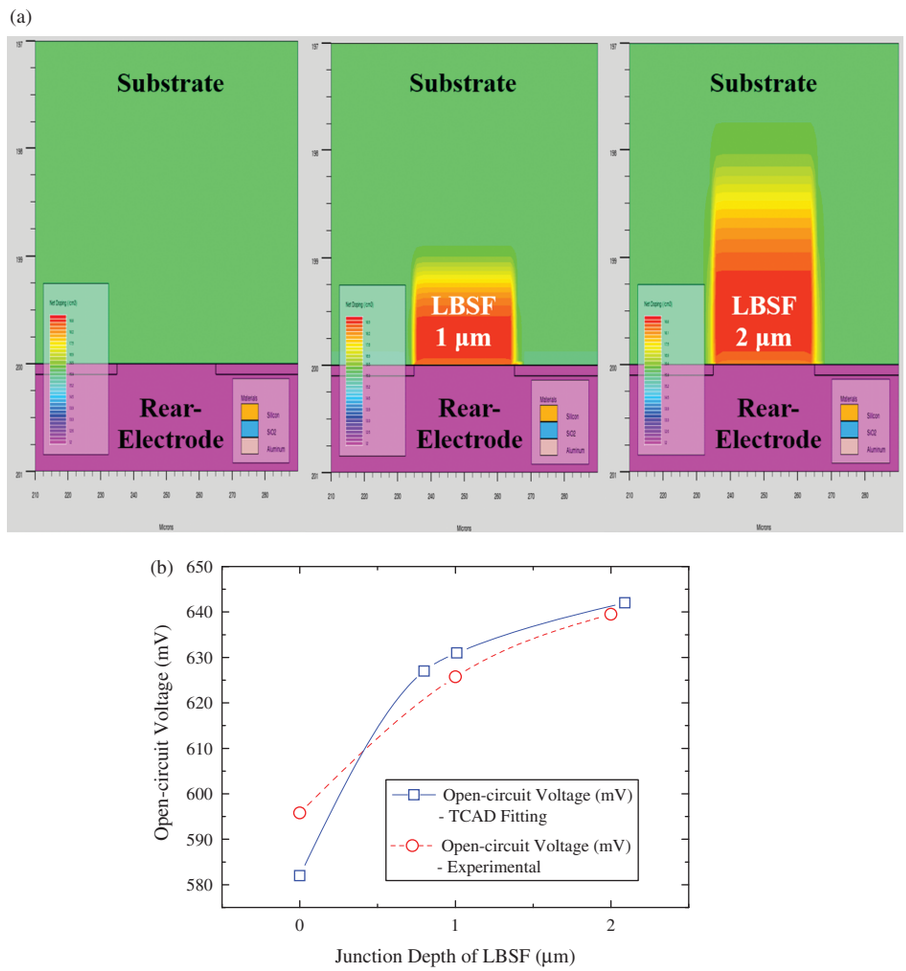

Figure 5. Simulated cell result by varying LBSF surface concentration.

contact pitch and W the sample thickness. In previous equations, SRV beneath the passivated area and metal contacts optimization was key issues for improving open-circuit voltage and rear-side effective SRV characteristics in locally contacted solar cells.

To analyze the quantitative distribution of components for the samples with different condition of laser fired frequency, EDS (Energy Dispersive Spectrometer) was measured. Figure 3 shows the EDS measurement results about relative material percentage variation of LBSF formed region by laser fired frequency. The Si/Al alloy was formed widely for the low frequency condition at which the local BSF was well formed. As the frequency was increased, the Si/Al alloy area became smaller compare than low laser frequency. This is the same trend as in the case of decreasing laser fired size verified through the optical microscope. The actual shapes of the dot formed under different conditions were observed with O.M. As the frequency increased, the diameter of the dot decreased as 35, 32, 29 and 27 μm when the laser power was 1%, Frequency from 10 kHz to 200 kHz. Laser spot region radius was reduced and shape of Si/Al relative material percentage was changed from "U" shape to "V" shape by laser frequency increased. LBSF characteristics by laser fired determined by Si/Al relative material percentage due to it means reaction ratio with Si and Al into laser spotted region. The results of contact resistance and LBSF junction depth characteristics by laser frequency was shown in previous figures. Lower laser frequency was shown good contact resistance and LBSF junction depth due to enough reaction between Si and Al to form LBSF.

Figure 4 shows the open-circuit voltage trends of the proposed structure with different LBSF layer thickness by laser frequency variation. The best open-circuit voltage obtained with the condition at which the local BSF well formed using 10 kHz frequency laser fired sample. The probability of recombination of electrons and holes lowered due to BSF. As a result, the SRV characteristics were improved and leakage current decreased. To improve the passivation effect by hydrogen diffusion, annealing was carried out in the environment of N_2 (95%) + H_2 (5%) forming gas at 450 °C for 25 minutes. After applying the FGA condition, open-circuit voltage measured again. It is found that open-circuit voltage improved for all samples. The values of V_{OC} varied from 642 mV to 575 mV depending on the laser conditions. Radius of laser spotted region and open-circuit voltage shows the same trend for the laser conditions. It was previously descripted in LV-SEM, S_{cont} and EDS measurement results, lower laser frequency providing well-formed Si/Al alloy LBSF by laser fired and higher open-circuit voltage.

Figure 5 shows the trend analysis between TCAD (Technology Computer Aided Design) simulation using SILVACO tool and experimental characteristics by proposed structure varying the junction depth of LBSF. Variation range of LBSF depth was changed from without LBSF to 2 μm refer to LV-SEM measurement results of laser fired samples. Simulated structure shown in Figure 5(a) using SILVACO TCAD tool. Concentration of LBSF was fixed to 2×10^{19} atoms/cm^2 due to Al solubility with silicon alloy. Figure 5(b) was shown open-circuit voltage characteristics by LBSF junction depth variation. Open-circuit voltage trend using TCAD simulation tool shows the same trend to experimental results by laser fired contact cells. Therefore, laser fired c-Si solar cell characteristics by laser condition variation was determined by LBSF thickness on rear-side.

The solar cell characteristics dependence on the back contact coverage and passivation was studied. The contact coverage varied as 0.1, 0.5, 0.9 and 1.5% using optimized laser fired condition (44 mW power, 10 kHz frequency). For each contact coverage samples with SRV of 20, 30 and 50 cm/s were compared. As the SRV decreases as shown in Figure 6(a), the V_{OC} increases after FGA as shown in Figure 6(b). The better passivation resulted in more collection of electrons and holes. However, when the contact coverage and SRV are considered, the contact coverage having better V_{OC} became larger as the SRV was higher. It is assumed that the collection of electrons and holes

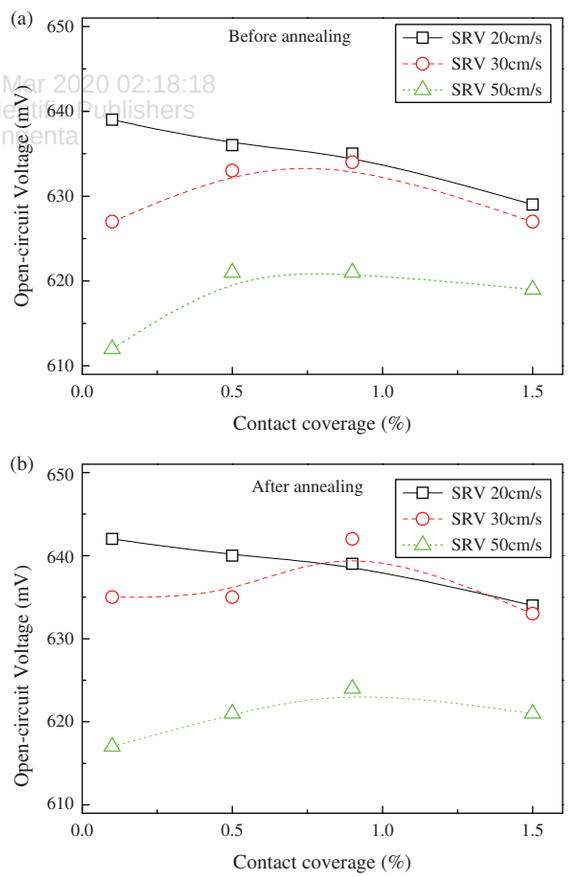

Figure 6. Rear contact coverage and passivation effects V_{OC} characteristics of solar cells based on (a) before FGA (b) after FGA.

decreased for the contact coverage that was out of the diffusion length.

4. CONCLUSION

The effects of back passivation and local BSF on the local back contact solar cells using laser fired contact were analyzed. Different passivation films of thermal SiO_2, additional FGA and SiN_x deposition by PECVD were compared by SRV characteristics. For both FGA and SiN_x deposition, the effect of passivation increased due to hydrogenation. Especially the SRV was 10∼30 cm/s with SiN_x deposition while it was 10∼30 cm/s when FGA was carried out.

The results showed that the samples with lower contact resistance had thicker LBSF and better passivation effect. When the solar cells were fabricated with the same laser conditions, the V_{OC} increased from 580 mV to 640 mV for the condition at which thick LBSF was formed well. The value of SRV was varied as 20, 30 and 50 cm/s. When it was 20 cm/s, V_{OC} was over 640 mV but it decreased to 610 mV with SRV of 50 cm/s.

In this paper, the importance of local BSF and the passivation quality on the back contact solar cells with laser fired contact were confirmed through both experimental and simulation results.

Acknowledgment: This work was supported by the Korea Institute of Energy Technology Evaluation and Planning (KETEP) and the Ministry of Trade, Industry and Energy (MOTIE) of the Republic of Korea (No. 20173010012940).

References and Notes

1. M. Tucci, E. Talgorn, L. Serenelli, E. Salza, M. Izzi, and P. Mangiapane, *Thin Solid Films* 516, 6767 (**2008**).
2. P. Ortega, A. Orpella, I. Martin, M. Colina, G. Lopez, C. Voz, M. I. Sanchez, C. Molpeceres, and R. Alcubilla, *Prog. Photovolt: Res. Appl.* 20, 173 (**2012**).
3. E. Schneiderlochner, R. Preu, R. Ludemann, and S. W. Glunz, *Prog. Photovolt: Res. Appl.* 10, 29 (**2002**).
4. U. Jager, D. Suwito, J. Benick, S. Janz, and R. Preu, *Thin Solid Films* 519, 3827 (**2011**).
5. U. Jager, M. Okanovic, M. Hortheis, A. Grohe, and R. Preu, *24th European PV Solar Energy Conference Proceeding* (**2009**), pp. 1740–1743.
6. B. G. Lee, Y. Lin, M. Sher, E. Mazur, and H. M. Branz, *38th Photovoltaic Specialists Conference (PVSC) Proceeding* (**2012**), pp. 1606–1608.
7. J. He, S. Hegedus, U. Das, Z. Shu, M. Bennett, L. Zhang, and R. Birkmire, *Prog. Photovoltaics Res. Appl.* 23, 1091 (**2015**).
8. A. Roigé, J. Alvarez, J. P. Kleider, I. Martín, R. Alcubilla, and L. F. Vega, *IEEE J. Photovolt.* 5, 545 (**2015**).
9. M. Ernst, D. Walter, A. Fell, B. Lim, and K. Weber, *IEEE J. Photovolt.* 6, 624 (**2016**).
10. M. J. Kerr, J. Schmidt, A. Cuevas, and J. H. Bultman, *J. Appl. Phys.* 89, 3821 (**2001**).
11. A. Wolf, D. Biro, J. Nekarda, S. Stump, A. Kimmerle, S. Mack, and R. Preu, *J. Appl. Phys.* 108, 124510 (**2010**).

Received: 6 April 2017. Accepted: 24 July 2017.